HHS Public Access

Author manuscript

Neurodegener Dis. Author manuscript; available in PMC 2017 January 01.

Published in final edited form as:

Neurodegener Dis. 2016 ; 16(1-2): 95–110. doi:10.1159/000440864.

AF710B, a Novel M1/σ1 Agonist with Therapeutic Efficacy in Animal Models of Alzheimer's disease

Abraham Fisher[1,2,✉,*], **Ilya Bezprozvanny**[3,4], **Lili Wu**[3], **Daniel A. Ryskamp**[3], **Nira Bar-Ner**[1], **Niva Natan**[1], **Rachel Brandeis**[1], **Hanoch Elkon**[1], **Victoria Nahum**[1], **Eitan Gershonov**[1], **Frank M. LaFerla**[5,6], and **Rodrigo Medeiros**[5,6]

[1]Israel Institute for Biological Research (IIBR), PO Box 19, Ness-Ziona, Israel

[2]Weizmann Institute of Science, Rehovot, Israel

[3]Department of Physiology, University of Texas Southwestern Medical Center, Dallas, TX 75390, USA

[4]Laboratory of Molecular Neurodegeneration, St. Petersburg State Polytechnical University, St. Petersburg 195251, Russia

[5]Department of Neurobiology & Behavior, University of California, Irvine (UCI), USA

[6]Institute for Memory Impairments and Neurological Disorders, University of California, Irvine (UCI), USA

Abstract

We previously developed orthosteric M1 muscarinic agonists (*e.g.*, AF102B, AF267B, and AF292), which act as cognitive enhancers and potential disease modifiers. We now report on a novel compound, AF710B, a highly potent and selective allosteric M1 muscarinic and σ1 receptor agonist. AF710B exhibits an allosteric agonistic profile on M1 muscarinic receptor; very low concentrations of AF710B significantly potentiated the binding and efficacy of carbachol on M1 receptors and their downstream effects (phopho-ERK1/2, phospho-CREB). AF710B (1–30 μg/kg, po) was a potent and safe cognitive enhancer in rats treated with the M1 antagonist trihexyphenidyl (passive avoidance impairment). These effects of AF710B involve σ1 receptor activation. In agreement with its anti-amnesic properties, AF710B (at 30 nM), via activation of M1 and a possible involvement of σ1 receptors, rescued mushroom synapse loss in PS1-KI and APP-KI neuronal cultures, while AF267B (1 μM) was less potent in PS1-KI and ineffective in APP-KI models, respectively. In female 3xTg-AD mice AF710B (10 μg/kg, ip/daily/2 months) – i) mitigated cognitive impairments in Morris water maze; ii) decreased BACE1, GSK3β activity, p25/CDK5, neuroinflammation, soluble and insoluble Aβ40, Aβ42, plaques and tau pathologies. AF710B differs from conventional σ1, M1 muscarinic (orthosteric, allosteric or bi-topic) or σ1/muscarinic agonists. These results highlight AF710B as a potential treatment for AD (*e.g.*, improving cognitive deficits, synaptic loss, amyloid and tau pathologies, and neuroinflammation) with a superior profile over a plethora of other therapeutic strategies.

✉**Corresponding Author:** Abraham Fisher, Ph.D., Address: Israel Institute for Biological Research, PO Box 19, Ness-Ziona 74100, Israel; Weizmann Institute of Science, Rehovot, Israel. fisher_a@netvision.net.il.
(*retired)
(academic adviser)

Keywords

M_1 mAChR; σ1R; Alzheimer's disease; AF710B; AF267B; AF series; cognitive deficits; memory; disease; modification; amyloids; tau; neuroinflammation

Introduction

Stimulation of the M1 muscarinic acetylcholine receptor (M1 mAChR) is an attractive therapeutic approach for Alzheimer disease (AD); reviewed in [1,2]. Accordingly, we recently generated compelling pre-clinical data, both pharmacology and genetically, that activation of M1 mAChR restores cognition and attenuates AD-like pathology in several animal models [3,4]. Mechanistically, it was found that M1 mAChR targets crucial enzymes involved in the synthesis of β-amyloid (Aβ) and phosphorylation of tau [1–4].

The sigma-1 receptor (σ1R) is another potential target for drug development for AD, as it is considered to play a fundamental role in cognitive function [5,6]. Notably, decreased levels of σ1R have been detected in early stage AD patients [7], and that stimulation of σ1R alleviates the depressive symptoms, neuronal cell death and cognitive deficits in AD mouse models [8,9]. Moreover, the mixed muscarinic/σ1R agonist ANAVEX2-73 resulted in significant inhibition of $A\beta_{25–35}$-induced tau phosphorylation and $A\beta_{1–42}$ seeding in mice [10] and was recently reported to exert positive cognitive effects in phase 2a clinical studies with AD patients (http://www.anavex.com/?post_type=news&p=1491).

σ1R is an endoplasmic reticulum (ER)-resident protein and a molecular chaperone, yet its functional role remains a mystery [5,6]. Under homeostatic conditions σ1R is concentrated at mitochondrial-associated membrane (MAM) junctions—sites of contact between ER and mitochondria—where it regulates $InsP_3R$-mediated calcium signaling and ER lipids [11]; however, agonists or ER stress can cause σ1R to exit the MAM domain [6], allowing it to regulate the function of plasma membrane ion channels [5] and G-protein coupled receptors (GPCRs) [6,8,12,13]. Among other brain regions, the σ1R is expressed in hippocampal neurons with preferential localization to plasmalemmal, outer mitochondrial and ER cisternal membranes within somata, dendrites and post-synaptic elements [14]. Ultrastructural analysis also shows colocalization of σ1R with mAChR in post-synaptic densities [15]. However, the mechanistic nature of σ1R's interactions with ion channels and GPCRs including mAChRs is poorly understood.

Over the past several years, our groups have focused on understanding the underlying molecular mechanism of M1 mAChR involvement in AD, and on development of innovative therapeutics to treat this insidious disease [1–4]. Thus we have created selective M1 mAChR orthosteric agonists in the "*AF series*" of compounds (e.g. AF102B, AF267B, AF292) that are cognitive enhancers and disease modifiers (reviewed in [1,2]):

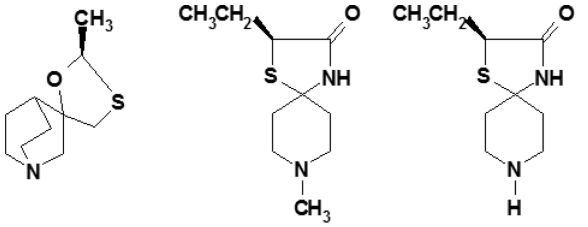

AF102B AF267B AF292

In a further expansion of our rational drug discovery programs we report here on AF710B, which is a novel and potent M1 mAChR/σ1R agonist:

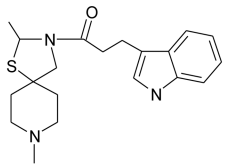

AF710B (active enantiomer of AF710); MW 357.5

We report here results of preclinical evaluation of AF710B in cellular and animal models of AD. Notably we found that AF710B showed exceptional efficacy in restoring cognitive decline associated with AD and with lessening BACE1, GSK3β activity, p25CDK5, neuroinflammation, soluble and insoluble Aβ40, Aβ42, accumulation of amyloid plaques and neurofibrillary tangles. As the stabilization of post-synaptic dendritic spines in hippocampal neurons is important for learning and memory, we evaluated the potential role of M1 mAChR and σ1R in the regulation of synaptic morphology. We recently found that mushroom spines are preferentially lost in PS1-M146V-knockin (KI) mouse [16] and APP-KI mouse [17] models of AD. As mushroom spines are considered stable “memory spines”, their loss may underlie cognitive decline in AD [16]. We therefore examined the effects of AF710B vs. AF267B on hippocampal mushroom spine stability and tested the involvement of M1 mAChR and σ1R in the mechanism of action of AF710B. The results of this study indicate that AF710B, but not AF267B, efficiently rescues mushroom spines and normalizes other pathological features in AD models.

Methods

Compounds

1-(2,8-Dimethyl-1-thia-3,8-diazaspiro[4.5]dec-3-yl)-3-(1H-indol-3-yl)propan-1-one (AF710); (US Patent 8,673,931B2) was synthesized at IIBR and was separated by Chiral Technology Europe into two enantiomers, AF710A and AF710B. AF710B {>99.5% chemical purity; >99.5% enantiomeric excess; specific rotation [α] = −56° (C=0.303, Methanol)}, the active enantiomer was used in the studies reported in this paper (re US Patent 8,673,931B2).

AF267B {(2S)-2-Ethyl-8-methyl-1-thia-4,8-diazaspiro[4.5]decan-3-one} (>99.9% chemical purity; > 99.5 enantiomeric excess) was provided by IIBR. All other compounds were of analytical grade and were purchased from commercial sources.

Receptogram profile in vitro

AF710B (10 μM) was tested in a high-throughput profiling that consists of a broad collection of 83 trans-membrane proteins (including GPCRs) and soluble receptors, sigma receptors, ion channels and monoamine transporters (CEREP, France; http://www.cerep.fr/cerep/users/pages/catalog/profiles/DetailProfile.asp?profile=2118). AF710B was further tested in binding studies at a wide concentrations range on M1 mAChR (IIBR; re below), σ1R receptors, σ2 receptors, α4β2, α7 nicotinic receptors as well as in cellular functional assays on histamine 2, 5HT2A, 5HT2C, 5HT2B, and mu receptors; and at 5- HT2B receptors in an *in vitro* rat stomach fundus bioassay, respectively (CEREP, France).

Animals (rats and mice)

All procedures in which animals were used were in accordance with i) the NIH Guide for the Care and Use of Laboratory Animals, (1996), and were approved by Israel Institute for Biological Research (IIBR), Institutional Animal Care and Use Committee; ii) the NIH guidelines and were approved by the Institutional Animal Care and Use Committee of the University of Texas Southwestern Medical Center; and iii) the Principles of Laboratory Animal Care from NIH publication 85–23 and were approved by the University of California, Irvine, Institutional Animal Care and Use Committee.

Binding studies to M1 mAChR in Rat Cortical Homogenates

Male Sprague Dawley rats, 250–300 gr, were sacrificed by decapitation and brains were removed. Cerebral cortex was dissected out and placed on ice, cleaned, weighed and transferred to 20 mM Tris-HCl buffer, 2mM EDTA, pH 7.4. The tissue was homogenized in the buffer (1:10 weight/volume) using a polytron homogenizer and after a −70°C freeze/thaw cycle; the homogenates were centrifuged at 35,000g at 4°C for 10 min. The supernatant were removed and the pellets were resuspended in Tris buffer at a ratio of 1:6 (weight/volume). The homogenates were divided into aliquots of 1 ml each and then stored at −70°C till use. The binding profile in rat cortical membranes of AF710B, carbachol and the effects of AF710B on carbachol binding to M1 mAChR, respectively, was studied in triplicates for each concentration of the tested compounds in displacement studies of the M_1 selective antagonist, [^{3}H]-pirenzepine ([^{3}H]PZ, 86 Ci/mmol, Perkin-Elmer, MA, USA). Each such study was replicated in 4–6 separate experiments. Competition curves, K_H, K_L and Ki values were derived using the GraphPad Prism software program, version 5.0.

Phospho-p44/42 MAPK (ERK 1/2) and phospho-CREB detection assay

Rat pheochromocytoma cells (PC12) stably transfected with rat M1 mAChR (PC12M1 cells) were seeded in 6-well plates at a density of 2×10^6 cells/well. The following day, cells were washed twice with RPM1, and returned to the incubator with serum free media (starvation medium containing RPMI, 2mM Glutamine, 1% penicillin- streptomycin, 2.5μg/ml Amphotericin B, 0.1 mg/ml G418). On the next day cells were pretreated for 3 hours with AF710B at concentrations ranging from 0.1nM to 100nM, and then carbachol (10nM) was added for 10 minutes. In each plate, one well served as a control (no treatment) and one well as a positive reference in which the cells were treated with carbachol (10nM). Following this procedure, cells were collected and extracted with Ripa buffer (Sigma,

R-0278, 200μl) containing a Protease inhibitor Cocktail (Sigma, 1:100) and Phenylmethylsulfonyl fluoride (Sigma, 1:1000). Phospho-p44/42 MAPK (p-ERK1/2) (1:1000, Cell signaling) and Phospho-CREB (ser 133) (1:1000, Cell signaling) were probed with anti-rabbit antibodies.

Passive avoidance (PA) studies in rats

Naive Wistar rats, 225–250 gr (3 months old) were trained and tested in a two-compartment box: a small illuminated compartment (21×23×22 cm^3) with a lamp (60w) at a height of 25 cm above the compartment, and a dark, large compartment (37×23×22 cm^3) equipped with grid floor. A door (7×5 cm^2) separated the two compartments. The PA task is comprised of a training (acquisition) phase and a retention phase. In the training procedure each rat was individually placed in the small illuminated compartment and after 60 sec of familiarization/adaptation, the door to the large compartment was opened and the latency to enter was measured (Initial latency). Immediately following entry into the dark compartment, the door was closed and an inescapable foot shock (0.6 mA for 3 sec) was delivered through the grid floor. A cutoff point of 180 sec was used for initial latency. Animals that failed to enter the dark compartment with all four paws within 180 sec were excluded from the experiment. After the acquisition trial the rat was returned to its home cage. Retention of the PA task was measured 24h later, by again placing the rat in the light compartment and after a 60 sec adaptation interval, the door was opened and the latency to re-enter the dark compartment was measured. A cutoff point of either 300 (*Experiments 1&2*) or 600 sec (*Experiment 3*) was used for retention latency. Animals that failed to step through within 300 or 600 sec were removed from the apparatus and a 300 or 600 sec latency was recorded for them.

In *Experiment 1* we tested the effects of AF710B [100, 30 and 10 μg/kg, per os (po)] and in *Experiment 2* lower doses (1 and 3 μg/kg, po). In both experiments the rats were divided into 2 groups. One main group was treated with trihexyphenidyl (5 mg/kg, s.c) and the second main group was treated with vehicle (DDW-1 ml/kg, s.c.), 30 min before the shock. In each main group, rats were further divided in treatment subgroups (N=9–11): one subgroup was treated with saline (10 ml/kg, p.o.), and the other subgroups were treated with AF710B, 60 min before the shock. *In Experiment 3* rats were divided into 2 groups. One group was treated with trihexyphenidyl (5 mg/kg, s.c), and the second group was treated with vehicle (DDW- 1ml/kg, s.c.), 30 min before the shock. In each group, rats were divided into treatment subgroups (N=9–10): one subgroup was treated with saline (10 ml/kg, p.o.), and the other subgroups were treated with AF710B (10 μg/kg, p.o.), with or without the σ1R antagonist, NE-100 (1mg/kg, po), 60 min before the shock.

Statistical analysis

Initial latency and retention latency were analyzed by a two-way MANOVA. Specific comparisons were made by simple main effects contrasts analysis.

Hippocampal primary neuronal cultures and spine morphology analysis

PS1-M146V knockin (PS1-KI) [18] and APP-KI [19] homozygous mouse AD models were used in our studies. Nontransgenic mice (WT) of the same strain (B6 strain) were used as a control. Primary hippocampal cultures from WT, PS1-KI and APP-KI mice were established

from postnatal day P0–P1 pups and maintained in culture as previously described [16,17,20]. At DIV7, hippocampal cultures were transfected with a TD-Tomato plasmid using a high calcium phosphate method [16]. At DIV16 neuronal cultures were treated with placebo (NBA medium), AF710B (30 nM) and AF267B (1 μM) for 16 hours. Following drug treatment the cultures were fixed (4% formaldehyde and 4% sucrose in PBS [pH 7.4]) for imaging. Z-stacks of optical sections were captured using a 100× objective with a confocal microscope (Carl Zeiss Axiovert 100M with LSM510). Quantitative analysis for dendritic spines was performed by using the NeuronStudio software package (as in [16]). In brief, following classification of spine shapes (thin, stubby, mushroom), the percentage of mushroom spines was calculated for each neurite. For each genotype and drug combination 12–20 cultured neurons were analyzed from at least 2 independent neuronal preparations. The data were pooled and averaged.

σ1R knockdown was achieved by lentiviral-mediated shRNA expression in hippocampal neurons. Bacteria containing plasmids encoding MISSION® shRNA targeting mouse σ1R (Clone ID:NM_011014.2-1138s21c1; Sequence: CCGGCCTGTAGTAATCTCTGGTGAACTCGAGTTCACCAGAGATTACTACAGGTTTTTG) or scrambled shRNA were ordered from Sigma-Aldrich. Plasmids were purified using a Maxi-prep (NucleoBond Xtra kit; Macherey-Nagel). After replacing culture media (DMEM + 10% FBS) with NBA, plasmids for shRNA along with plasmids for Δ8.9 and VSVG for lenti-viral production and packaging were transfected into HEK293 cells using PEI. Culture media was collected 48 hours after transfection, centrifuged (2000 RPM for 5 min), filtered (0.45 μm pore size) and aliquoted in cryotubes for storage at −80°C until use. 200 μl of the collected lenti-virus media was added to each well of neuron cultures on DIV8. Both functional analysis in the spine loss assay and SDS-PAGE western blot analyis of lysates from neurons cultures (using σ1R (SC-137075; Santa Cruz) and β-tubulin (E7; DSHB) antibodies and the immunoblotting protocol below) confirmed efficient knockdown by si-σ1R.

Studies in 3xTgAD

3xTgAD mice harboring a presenilin1 mutation ($PS1_{M146V}$), the Swedish double mutation in APP ($APP_{KM670/671ML}$), and a frontotemporal dementia mutation in tau (tau_{P301L}) were used for all experiments [21]. Strain matched nontransgenic mice (nTg), 129/C57BL/6, were used as controls. AF710B was administrated via intraperitoneal (ip) injection at dose of 10 μg/kg/day. Mice were treated for 2 months, from 10 months of age to 12 months of age. No changes in body weight were found between vehicle- and AF710B-treated mice.

Morris water maze

Behavior paradigms to assess cognition were performed for all groups of mice two weeks before sacrifice as described previously [4]. Mice were trained to swim to a circular clear Plexiglas platform submerged 1.5 cm beneath the surface. Four trials were performed per day, for 60 seconds each with 5 minutes between trials. Mice were trained for as many days as needed for the group to reach the training criterion of 25 seconds. The probe test was assessed 24 hours after the last trial, with the platform removed. Performance was monitored

with the EthoVision XT video-tracking system (Noldus Information Technology, Leesburg, VA, USA).

Tissue preparation

Mice were deeply anesthetized with sodium pentobarbital and killed by perfusion transcardially with 0.1 M phosphate-buffered saline (PBS, pH 7.4) solution. The right brain hemispheres were fixed for 48 hours in 4% paraformaldehyde and cryoprotected in 30% sucrose for immunohistochemical analysis. Frozen brains were sectioned coronally into 40 μm sections using a Leica SM2010R freezing microtome, serially collected in cold 0.02% sodium azide and stored at 4°C. The left hemispheres were snap-frozen on dry ice and subject to protein extraction sequentially using T-PER tissue protein extraction reagent (Thermo Scientific, Rockford, IL, USA) and 70% formic acid. The supernatant was aliquoted and stored at −80°C. Protein concentration in the supernatant was determined using the Bradford assay.

Immunoblotting

Equal protein amounts were separated on a 4–12% gradient SDS-PAGE, transferred to a nitrocellulose membrane and incubated overnight at 4°C with primary antibody. The following primary antibodies were used in this study: anti-$A\beta_{1-16}$ (6E10) (Covance Research Products) phospho-GSK3β (Ser^{9}), human APP-CT20, ADAM10, ADAM17, BACE1, GSK3β, CDK5 (Calbiochem, San Diego, CA, USA), human Tau (HT7), phospho-Tau AT180 (phospho-Thr^{231}), phospho-Tau AT270 (phospho-Thr^{181}) (Thermo Scientific), PP2A, p35, GAPDH (Sigma- Aldrich, St. Louis, MO, USA) and phospho-Tau PHF-1 (phospho-S^{396}/S^{404}) (Dr. Peter Davies, Albert Einstein College of Medicine, Manhasset, NY, USA). Following washing, the membranes were incubated with adjusted secondary antibodies coupled to horseradish peroxidase. The immunocomplexes were visualized using the SuperSignal West Pico Kit (Thermo Scientific). Band density measurements were made using ImageJ 1.36b imaging software (NIH, Bethesda, MD, USA).

Enzyme-Linked Immunosorbent Assay (ELISA)

For the determination of the Aβ levels, T-Per soluble fractions were loaded directly onto ELISA plates, whereas the formic acid supernatants (insoluble fractions) were diluted 1:20 in a neutralization buffer (1 M Tris base, 0.5 M NaH_2PO_4) before loading. MaxiSorp immunoplates (Nunc, Rochester, NY, USA) were coated with mAb20.1 antibody (Dr. William E. Van Nostrand, Stony Brook University, Stony Brook, NY, USA) at a concentration of 25 μg/ml in coating buffer (0.1 M Na_2CO_3, pH 9.6) and blocked with 3% bovine serum albumin. Standard solutions for both $A\beta_{40}$ and $A\beta_{42}$ were made in the antigen capture buffer (20 mM NaH_2PO_4, 2 mM EDTA, 0.4 M NaCl, 0.05% 3-[(3-cholamidopropyl)dimethylammonio]propane sulfonate, and 1% bovine serum albumin, pH 7.0) and loaded onto ELISA plates in duplicate. Samples were then loaded (also in duplicate) and incubated overnight at 4°C. Plates were then washed and probed with either horseradish peroxidase-conjugated anti-$A\beta_{40}$ (C49) or anti-$A\beta_{42}$ (D32) (Dr. Vitaly Vasilevko and Dr. David H. Cribbs, University of California Irvine, CA, USA) overnight at 4°C. The chromogen was 3,3',5,5'-tetramethylbenzidine, and the reaction was stopped by 30% phosphoric acid. The plates were read at 450 nm using a plate reader (Molecular

Dynamics, Sunnyvale, CA, USA). The readings were then normalized to protein concentrations of the samples.

Immunohistochemistry

Free-floating sections were pre-treated with 3% hydrogen peroxide and 10% methanol in Tris-buffered saline (TBS) for 30 min to block endogenous peroxidase activity. After a TBS wash, sections were incubated once in 0.1% Triton X-100 in TBS (TBST) for 15 min and once with 2% bovine serum albumin (BSA) in TBST for 30 min. Sections were then incubated overnight at 4°C with phospho-Tau AT8 (phospho-Ser^{212}/Thr^{214}, Thermo Scientific) with 5% normal serum in TBS. After the appropriate biotinylated secondary antibody (1:200 in TBS + 2% BSA + 5% normal serum), sections were processed using the Vectastain Elite ABC reagent and 3,3'-diaminobenzidine (Vector Laboratories, Burlingame, CA, USA) according to the manufacturer's instructions. Sections were then mounted on gelatin-coated slides, dehydrated in graded ethanol, cleared in xylene and coverslipped with DPX mounting medium (BDH Laboratory Supplies, Poole, England).

The immunostaining was assessed at six brain coronal levels. Specifically, six alternate 40-μm sections of the brain with an individual distance of ~160 μm were obtained between 1.34 and 2.54 mm posterior to the bregma. Images of stained hippocampal area were acquired using an Axiocam digital camera and AxioVision 4.6 software connected to an Axioskop 50 microscope (Carl Zeiss MicroImaging, Thornwood, NY, USA). A threshold optical density that best discriminated staining from the background was obtained using the ImageJ 1.36b imaging software (NIH). All histological assessments were made by an examiner blinded to sample identities.

Immunofluorescence

Sections were first blocked with 3% normal serum, 2% bovine serum albumin and 0.1% Triton X-100 in TBS for 1 hr at room temperature. Using the same buffer solution, sections were incubated overnight at 4°C with the following primary antibodies: anti-A$\beta_{1–16}$ (6E10) (Covance Research Products, Denver, PA, USA), anti-Iba-1, anti-GFAP (Millipore, Billerica, MA, USA), Human tau (HT7) and/or phospho-Tau AT8 (phospho-Ser^{202}/Thr^{205}) (Thermo Scientific). Sections were then rinsed and incubated for 1 hour with secondary Alexa Fluor-conjugated antibodies (Invitrogen, Carlsbad, CA, USA) at room temperature. Finally, sections were mounted onto gelatin-coated slides in Fluoromount-G (Southern Biotech, Birmingham, AL, USA) and examined under a Leica DM2500 confocal laser microscope using the Leica Application Suite Advanced Fluorescence software (Leica Microsystems, Bannockburn, IL, USA). The immunofluorescence was assessed at the same brain coronal levels described above. Confocal images were acquired by sequential scanning using a z-separation of 1 μm using the Leica Application Suite Advanced Fluorescence software (Leica Microsystems).

Thioflavin S staining

Sections were incubated in 0.5% thioflavin S in 50% ethanol for 10 min, differentiated twice in 50% ethanol, and washed in PBS solution. Staining was visualized under a confocal microscope. Volumetric imaging and image measurements were made using Imaris software

(Bitplane Inc., South Windsor, CT, USA). The thioflavin S levels represent the average value obtained by the analysis of images of the hippocampus.

Statistical Analysis

All data are expressed as mean ± SEM. The statistical evaluation of the results was carried out using one- or two-way analysis of variance (ANOVA). Following significant ANOVAs, multiple post hoc comparisons were performed using Bonferroni's test. Some data were analyzed using the unpaired t-test. The accepted level of significance for the tests was $P < 0.05$. All tests were performed using the Statistica software package (StatSoft Inc., Tulsa, OK, USA).

Results

AF710B shows high potency and selectivity to M1 mAChR and σ1R

In high-throughput receptogram profiling AF710B emerged as a potent ligand for M1 mAChR and σ1R, respectively, as shown by displacement of an M1 muscarinic antagonist (tritiated-pirenzepine; an M1 mAChR radioligand) from rat cerebral cortex and of a σ1R agonist (tritiated-pentazocine; a σ1R radioligand) from guinea-pig cerebral cortex with a 6- and 2-fold order of magnitude interval between two binding sites (K_H vs. K_L), respectively (Fig 1A). Furthermore AF710B showed both high potency and selectivity for the M1 mAChR and σ1R and very clean additional pharmacological profiles with regard to off-target activity (Fig 1A). Thus AF710B was found to display no significant off-target activity when screened at 10 μM in a radioligand displacement screen at 83 other GPCRs, ion channels and transporters known to mediate human side effects (Fig 1A). AF710B (10 nM-100 μM) was inactive as an agonist or an antagonist on histamine 2 and 5HT2A & 5HT2C receptors while on 5HT2B receptor it is a very weak partial agonist (17% efficacy) at 100 μM; and a very weak agonist at mu receptor, EC50=13 μM. Additionally, AF710B (0.1nM-10 μM) did not bind to human α4β2 and α7 nicotinic receptors and to σ2R, while it showed agonistic effects on M1 mAChR, but not on M2–M5 mAChR (Table 1). In addition, AF710B application altered the neurochemical profile to a state typified by downstream signaling of M1 mAChR and/or σ1R. This was detected at concentrations in the nM range ~3–4 orders of magnitude lower than effects on other screened GPCRs, ion channels and transporters mentioned above (detailed data not shown, Table 1).

To characterize the interaction of AF710B with the M1 mAChR we employed a combination of binding and functional assays. This was done first utilizing brucine, an M1 positive allosteric modulator (M1 PAM) that potentiates M1 orthosteric, but not M1 allosteric agonists [22]. Notably while brucine showed a modest cooperativity on M1 mAChR with the orthosteric agonists, carbachol and AF267B, it failed to potentiate AF710B (tested in binding and calcium mobilization assays) and TBPB (another M1 allosteric agonist, [23]); (detailed data not shown; Table 1). Thus, AF710B binds to M1 mAChR on a location different from the orthosteric site, supporting an allosteric mechanism of action of AF710B.

To further characterize the M1 allosteric profile of AF710B we tested its effects on carbachol. AF710B (0.1 nM) potentiated carbachol binding to M1 mAChR in rat cortical membranes as evidenced by a decrease by ca. two orders of magnitudes of the K_H for carbachol. The ratio of K_L/K_H for a given agonist directly correlates with its efficacy. In this particular case, the ratio of K_L/K_H for carbachol in presence of AF710B 0.1 nM increased from 110 to 1650 (Fig 1B). Thus both the affinity and efficacy of carbachol are potentiated by AF710B.

Both M1 orthosteric and allosteric agonists increase phosphorylation of extracellular signal regulated kinase (ERK 1/2) [24,25]. The activated ERK/ mitogen activated protein kinase (MAPK) cascade has multiple targets, including cAMP response element binding protein (CREB), which mediates its ability to induce memory consolidation and long-term memory formation [26,27]. In this context we found that AF710B did not increase phopho-ERK1/2, yet it potentiated ERK 1/2 phosphorylation induced by 10 nM carbachol (Fig 1C). In addition AF710B increased carbachol-induced pCREB in starved proliferated PC12M1 cells (Fig 1D).

Taken together this indicates that AF710B is functioning like an M1 PAM mAChR. However, unlike reported M1 PAMs [23] AF710B binds to M1 mAChR with a high affinity and is also a direct M1 allosteric agonist, but different in several aspects from other reported M1 allosteric agonists (*vide infra* and Table 1).

AF710B reverses the cognitive decline induced by M1 mAChR antagonist, trihexyphenidyl via activation of both M1 mAChR and σ1R

To determine whether AF710B is a cognitive enhancer we tested its effects against cognitive impairments in a passive avoidance (PA) test induced by trihexyphenidyl in rats. Trihexyphenidyl induces cognitive deficits in rodents and humans and is a CNS penetrating and a relatively selective M1 antagonist [28].

In general, no significant difference was found in initial latency between any of the groups tested in *Experiments 1–3* (data not shown*)*. In *Experiment 1* a significant interaction was found between trihexyphenidyl and treatments ($F(2/63)=4.0$, $p<0.023$). Retention latency of trihexyphenidyl rats treated with double distilled water, DDW (54.2±14.6sec) was significantly shorter than that of control rats treated with DDW (242.00±30.60 sec) ($p<0.001$). However, the retention latency of trihexyphenidyl rats treated with AF710B- 10, and 30 μg/kg (po) was significantly longer than that of trihexyphenidyl rats treated with DDW ($p<0.001$–0.01). The retention latency of trihexyphenidyl rats treated with AF710B-100 μg/kg, po was not different from that of trihexyphenidyl rats treated with DDW. AF710B-10 μg/kg was very potent, and significantly different from the higher dosage of 100 μg/kg, po ($p<0.01$). In *Experiment 2* a significant interaction was found between trihexyphenidyl and treatments ($F(2/52)=5.2$, $p<0.009$). Retention latency of trihexyphenidyl rats treated with DDW (63.9±18.8sec) was significantly shorter than that of control rats treated with DDW (274.7±20.8sec) ($p<0.001$). However, the retention latency of trihexyphenidyl rats treated with AF710B (1 and 3 μg/kg, po), were significantly longer than that of trihexyphenidyl rats treated with DDW ($p<0.001$). The antiamnesic effects AF710B, 1 and 10 μg/kg (po), were replicated two and four times, respectively and the tested

compound showed a long duration of action at these doses, since the retention time was significantly different vs. DDW treated trihexyphenidyl-rats, both 24 after 72 hours, after treatment (detailed data not shown).

As AF710B binds to both M1 mAChR and σ1R we explored whether its anti-amnesic effects are blocked by NE-100, a selective σ1R antagonist [29]. In *Experiment 3* we found that the retention latency of trihexyphenidyl rats treated with DDW (122.0±29.2sec) was significantly shorter than that of control rats treated with DDW (525.7±51.0 sec) ($p<0.001$). However, the retention latency of trihexyphenidyl rats treated with AF710B 10μg/kg, po was significantly longer (361.7±67.1 sec) and NE-100 co-administered with AF710B, blocked significantly the anti-amnesic effect of AF710B in this model (185.4±44.0 sec) ($p<0.02$); (Fig 1F). Thus the effects of AF710B appear to be mediated at least in part by the σ1R. Notably, NE-100 was not significantly effective in inducing deficits in the PA task and also failed to affect the retention parameters of AF710B alone (Fig 1F). As trihexyphenidyl binds 70 fold more effectively to M1 mAChR vs. σ1R [30] and its amnesic effects may be attributed mainly to its M1 antagonistic effects, it can be deduced that AF710B exerts its cognitive effects in the trihexyphenidyl model *via* a combined activation of both M1 mAChR and σ1R.

AF710B protects synapses via activation of M1 mAChR/σ1R

Synaptic loss is a main feature of many neurodegenerative disorders, including AD [31]. In previous studies we determined that mushroom synaptic spines are lost in primary hippocampal neuronal cultures from PS1-KI and APP-KI mice [16,17]. We confirmed these findings in the present experiments (Figs 2A–D). Application of AF267B (1μM, an effective concentration on M1 mAChR- mediated readouts; [2]) for 16 hours starting on day *in vitro* (DIV) 16 partially rescued mushroom spines in PS1-M146V.KI cultures, but not in APP.KI cultures (Figs 2A–B), indicating potential beneficial effects, but only for certain forms of AD. AF267B partially reduced the prevalence of WT mushroom spines, which could be related to a slight toxic effect or depression of synaptic strength. By contrast, 30 nM AF710B did not change the proportion of mushroom spines in hippocampal cultures from non-transgenic (nTg) animals when compared with vehicle, (Fig. 2A, 1B). Notably, AF710B markedly rescued mushroom spine loss in both AD transgenic mouse models, nearly to the level of non-transgenic animals (Fig. 2A,B), indicating that this compound exerts a disease-modifying effect on AD neurons.

To explore the underlying molecular mechanism responsible for AF710B's protective effect, similar studies with primary hippocampal cultures from APP-KI mice were performed in the presence of the M1 mAChR antagonist pirenzepine (1 μM) and/or the σ1R antagonist NE100 (1 μM) (Fig 2C). While the effect of AF710B on spine morphology was not affected by the blockage of σ1R, it was completely abolished in the presence of the M1 mAChR antagonist (Fig 2C, 2D). In addition, the combination of pirenzepine and NE100 did not show any additive or synergistic effects in the presence of AF710B (Figs. 2C, 2D). These results suggest that AF710B prevents mushroom spine loss in hippocampal neuron cultures from APP-KI mice by stimulating M1 mAChR activity.

We further examined the possible involvement of σ1R in mushroom spine stability in WT mouse hippocampal neuronal cultures by using lentiviral-mediated shRNAi delivery. σ1R knockdown decreased the mushroom spine density from 38.4 ± 1.1% in hippocampal neurons transfected with scrambled siRNA to 22.1 ± 1%, significantly lower ($p < 0.0001$; Fig. 2E,F). As before, treatment of cultures with 30 nM AF710B for 16 hours had no effect on the mushroom spine density in control-siRNA expressing neurons (Fig. 2E,F). However, AF710B treatment failed to rescue mushroom spine loss in hippocampal neurons expressing siRNA against σ1R (si-σ1R) (Fig. 2E,F), indicating that ability of AF710B to stabilize hippocampal mushroom spines requires not only M1 mAChR function, but also σ1R expression. To explain these results we propose that AF710B may act by stimulating a M1 mAChR/σ1R complex in the synaptic spines. Further biochemical experiments will be needed to test this hypothesis.

AF710B mitigates cognitive impairments in the 3xTg-AD mouse model

Given the marked effects induced by AF710B *in vitro* and *in vivo*, we sought to further investigate its effects on the cognitive decline induced by AD using the 3xTg-AD mouse model. As previously observed, 12-month-old 3xTg-AD mice performed significantly worse relative to age-matched nTg mice in the reference spatial memory version of the Morris water maze (MWM). Vehicle-treated 3xTg-AD mice exhibited longer latencies to find the platform in the training session (Fig. 3A) and reduced target quadrant preference during the probe trial (Fig. 3B) compared with age-matched nTg mice treated with vehicle. Notably, treatment with AF710B (10 μg/kg/day, ip, for two months) improved the cognitive function of 3xTg-AD mice during the training and probe sessions of the MWM (Fig. 3A,B). Importantly, the improvement in the cognitive performance in the AF710B-treated 3xTgAD mice are not directly related to changes in motor function, since no significant alterations of the swimming speed and total distance travelled in the water maze were observed when compared with vehicle-treated nTg and 3xTgAD mice (data not shown).

AF710B lessens AD-like pathology in the 3xTg-AD mouse model

Accumulation of Aβ and tau pathology coincides with the synaptic loss and cognitive decline in the 3xTgAD mice. Therefore, we next examined for changes in Aβ pathology. We found that AF710B treatment significantly reduced levels of $Aβ_{40}$ and $Aβ_{42}$, in both detergent soluble and insoluble fractions (Fig. 3C). Moreover, we found significantly less amyloid deposition in the AF710B-treated animals versus vehicle-treated animals, as indicated by the significant decrease in Thioflavin S positive plaques (Fig. 3D). To elucidate the mechanism by which AF710B reduces Aβ levels, we determined whether APP processing pathways were modified (Fig. 3E). Steady-state levels of APP and α-APP cleaving enzymes ADAM10 and ADAM17 were unaffected by AF710B treatment. Conversely, AF710B significantly diminished the expression of the putative β-secretase enzyme BACE1. Given the decline in BACE1 levels, we used the antibody 6E10 to detect full-length APP and its proteolytic fragments CTFβ [99-amino-acid long C-terminal APP fragment produced by β-secretase cleavage (C99)] and CTFα [83-amino-acid long C-terminal APP fragment produced by α-secretase cleavage (C83)]. As expected, the levels of C99, but not C83, were significantly diminished in the AF710B-treated 3xTgAD mice versus vehicle-treated 3xTgAD mice.

To examine the effect of AF710B administration on tau pathology, we first tested for changes in total phosphorylated-tau (p-tau) levels using the anti-AT100 antibody. Notably, p-tau was found reduced in AF710B-treated 3xTgAD mice versus vehicle-treated 3xTgAD mice (Fig. 3F). This data was further confirmed through confocal studies, which showed a reduction in AT8-positive neurons in AF710B-treated 3xTg-AD mice (Fig. 3G). Biochemical analysis of p-tau revealed significant decreases in the p-tau epitopes AT180, AT270, and PHF-1 (Fig. 3H). To determine if the reductions in p-tau levels were due to modulations in tau kinase function, we measured for changes in several kinases involved in tau phosphorylation. We found that AF710B administration significantly increased phosphorylation in GSK3β, at the inhibitory Serine-9 residue (Fig. 3H). This was also associated with an effect on p35 cleavage, since the brains of AF710B-treated 3xTgAD mice presented diminished levels of p25 fragment. However, AF710B did not affect the steady state levels of CDK5, GSK3β or PP2A. Overall, our data indicates that AF710B modulates tau pathology via the modulation of GSK3β and CDK5 activities.

Inflammation is another critical component of AD, and it is associated with increased numbers and/or size of microglia and astrocytes. We found significantly less reactive astrocytes and activated microglia in AF710B-treated animals, as indicated by the lower detection of GFAP and Iba-1, respectively. This anti-inflammatory effect was most prominent in the immediate vicinity of plaques. The immunofluorescence studies indicated lower amyloid load and glial reactivity (Fig. 3I).

Discussion

We report here on AF710B, which is a novel and highly potent mixed M1 mAChR/σ1R agonist with a unique mechanism of action leading to a concomitant activation of both M1 mAChR and σ1R. Notably, AF710B showed both high potency and selectivity for the M1 mAChR and σ1R and very clean additional pharmacological profiles with regard to off-target activity (Fig 1A and Table 1). AF710B exhibits an allosteric agonistic profile on M1 mAChR since very low concentrations of AF710B significantly potentiated the binding and efficacy of carbachol on M1 mAChR and some of the carbachol/M1- mediated downstream effects (e.g., ERK1/2 and CREB phosphorylation); Fig 1B–D. Furthermore, AF710B showed exceptional efficacy *in vitro* on downstream effects mediated by M1 mAChR and σ1R including ability to preserve synaptic elements (Fig 2), and *in vivo* in restoring cognitive deficits in animal models (trihexyphenidyl treated rats and 3xTg-AD mice) and with lessening major hallmarks associated with AD such as BACE1, GSK3β activity, p25/CDK5, neuroinflammation, soluble and insoluble Aβ40, Aβ42, accumulation of amyloid plaques and neurofibrillary tangles (in 3xTg-AD mice) (Fig 1 and 3 and Table 1).

While pK studies were not yet performed on AF710B, its exceptional brain penetration and target engagement can be implied from the very high potency of the compound in *in vivo* studies. Notably, AF710B functions as a cognitive enhancer in the PA test involving trihexyphenidyl-treated rats at unprecedented low doses of 1–30μg/kg, po (Fig 1E). The effects of AF710B on cognition are enantioselective since the enantiomer AF710A is not active at 1 and 10 μg/kg, po (Table 1 and 2A). Strong enantioselectivity of AF710B vs. AF710A was consistently observed *in vitro* and *in vivo* (Table 1). How does AF710B

pharmacodynamics overcome existing compounds? We found that AF710B is the most potent cognitive enhancer and with the highest safety margin vs. a variety of compounds tested by us in the trihexyphenidyl model under same experimental protocols as tested for AF710B, including, *inter alia*, AF710A, AF102B, AF267B, AF292 and donepezil (Table 2A).

To explore the mechanism of action *in vivo* of AF710B in ameliorating PA impairments induced by trihexyphenidyl we used NE-100, a selective σ1R antagonist [29]. We found that NE-100 co-administered with AF710B, significantly blocked the anti-amnesic effect of AF710B in this model (Fig 1F). Thus, the effects of AF710B appear to be mediated in part by the σ1R. However, NE-100 was not significantly effective in inducing deficits in the PA task and also failed to affect the retention parameters of AF710B alone (Fig 1F). As trihexyphenidyl binds to M1 mAChR > σ1R [30] and its amnesic effects may be attributed mainly to its M1 antagonistic effects, it can be implied that AF710B exerts its cognitive effects in the trihexyphenidyl model *via* a unique concomitant activation of both M1 mAChR and σ1R.

Can such effects of AF710B be recapitulated with a mixture of separate agents acting on M1 mAChR and σ1R, respectively? We tested this in the trihexyphenidyl model *via* a combined treatment of the M1 orthosteric agonist (AF267B) with donepezil. Notably the acetylcholinesterase inhibitor (AChE-I) donepezil, the current major treatment in AD patient, is also a potent σ1R agonist and its effects may arise from cholinergic mechanisms, as well as an interaction with the σ1R [32]. Importantly we found that the effects of AF710B could not be recapitulated by the combination of AF267B + donepezil as no significant potentiation was detected and in fact the beneficial effects of the M1 agonist were unchanged by donepezil (Table 2A). Thus it can be deduced that the mechanism of action of AF710B differs from a combination of a direct acting M1 orthosteric agonist and σ1R agonist.

As AF710B potentiated the effects of carbachol on three tested readouts (*e.g.*, binding, phopho-ERK1/2, phospho-CREB; Fig 1B–D), it is possible that the affinity and efficacy of the endogenous agonist, acetylcholine, for the M1 mAChR is also potentiated by AF710B, which may explain improved memory performance in trihexyphenidyl-treated rat and 3xTg-AD mice models. These findings already separate AF710B from M1 orthosteric agonists [e.g. AF267B, AF292, AF102B and others] or from σ1R agonists. Supersensitive M1 receptors are induced by positive M1 PAMs that are currently under examinations by several major drug companies [23]. These M1 PAMs potentiate the whole repertoire of acetylcholine-induced M1 mAChR-mediated downstream responses, including release of intracellular Ca^{2+}, $[Ca^{2+}]i$. In contrast, AF710B diverges mechanistically from other M1 PAMs and M1 agonists (allosteric or orthosteric) in *in vitro studies* and in spite of inducing a supersensitive M1 mAChR, it does not potentiate carbachol-mediated release of $[Ca^{2+}]i$ (detailed data not shown, Table 1). Notably, orthosteric, allosteric or bi-topic M1 agonists increase $[Ca^{2+}]i$ at the same concentration range that these compounds induce other downstream signaling. This is not the case for AF710B and therefore this compound diverges mechanistically from M1 orthosteric agonists (*e.g.*, AF267B, AF102B, AF292, and more; [1,2]), M1 allosteric agonists (*e.g.*, TBPB, and more), or M1 PAMs (BQCA, Brucine

and more; [23]); (detailed data not shown, Table 1). Interestingly, unlike AF710B, M1 PAMs and M1 agonists (allosteric or orthosteric) were not reported to have σ1R activity. In addition, reported M1 PAMs or M1 allosteric agonists (or bi-topic M1 agonists) are effective as cognitive enhancers at doses >1mg/kg, unlike AF710B (effective at μg/kg range). Thus, AF710B exhibits a remarkably different mechanism of action vs. and superior profile vs. all these compounds.

Results from drug screening and the trihexyphenidyl model implied that AF710B might improve memory by combined activation of M1 mAChR and σ1R. As hippocampal mushroom spine loss may underlie memory deficits in AD [16], we tested a potential role for AF710B in stabilizing synaptic connections and found that AF710B rescues mushroom spine loss *in vitro* in PS-KI and APP-KI hippocampal cell culture models of AD. Considering the established role of σ1R as a sensor of ER Ca^{2+} dysregulation [11] and the deranged ER Ca^{2+} signaling in AD neurons [16,20], it is likely that σ1R activity is abnormal in spines of AD neurons. Indeed, σ1R agonists affect learning and memory, cognition and mood and show potent anti-amnesic properties [8] and σ1R knockdown causes hippocampal spine loss [33]. Additionally, σ1R agonists may have therapeutic potential in protein conformation diseases (e.g. AD. PD and more) and several neuropsychiatric disorders [8]. Conversely, σ1R KO mice are viable, but have a late-onset neurodegeneration phenotype [15]. Thus, it appears that partial loss of σ1R function or reduction in its expression may contribute to synaptic impairment and neuronal loss in these disorders. We therefore tested the potential involvement of σ1R in mediating the neuroprotective effects of AF710B. Although the σ1R antagonist NE100 did not block the rescue of mushroom spines by AF710B in hippocampal neurons from APPKI mice, inhibition of M1 mAChR prevented the rescue by AF710B. However, σ1R knockdown in wild type hippocampal neuron cultures compromised mushroom spine stability and AF710B treatment was unable to prevent this, indicating requirements for both σ1R and M1 mAChR activity in hippocampal mushroom spine stability. To explain these results we propose that AF710B may act by stimulating a M1 mAChR/σ1R complex in the synaptic spines. Notably, heteromers constituted by σ1Rs with D1Rs or D2Rs (both GPCRs) were reported [12,13] and it is reasonable to presume that other GPCRs, including the M1 mAChR, may also form heteromers with σ1R. Further biochemical experiments will be needed to test this hypothesis.

The hypothesis that AF710B targets a putative M1 mAChR-σ1R complex may be tied with the pro-cognitive effects of AF710B at unprecedented low doses in memory-based behavioral tasks in both trihexyphenidyl-treated rats (Fig 1E and F; Table 2A) and 3xTgAD mice (Fig. 3A,B and Table 2B). In this context, in the 3xTg-AD mice AF710B mitigated cognitive deficits, and decreased BACE1 levels, GSK3β and p25CDK5 activity, neuroinflammation, soluble and insoluble Aβ40 and Aβ42 plaques, and tau pathology (Fig. 3). Furthermore, unlike the remarkable disease-modifying properties found with AF710B in 3xTg-AD mice at very low doses (10μg/kg/day, ip, for 2 months), no *in vivo* disease-modifying properties were reported for M1 PAMs or M1 allosteric agoinsts and M1 dualsteric agonists in Tg mice or in other *in vivo* models [2,23].

Glycogen synthase kinase 3β (GSK3β) and cyclin-dependent kinase 5 (CDK5) contribute to hyperphosphorylation of tau protein, one of the pathological hallmarks of the disease

(reviewed in [34]). Cdk5 activity is increased in AD patients, probably due to the conversion of the Cdk5 activator p35 to the truncated p25 protein (reviewed by [34]). Elevated p25 levels are observed in AD patients [35]. CDK5 activator protein p25 preferentially binds and activates GSK3β [36]. All these data supported the hypothesis that Cdk5/p25 acts as a master regulator of neuronal cell death in AD, Parkinson's disease and several neurodegenerative diseases, [34]. Interestingly, activation of the M1 mAChR decreased several phosho-tau isoforms via GSK3β inhibition but not the phosho-tau isoform detected with PHF-1 [3], while activation of σ1R help maintain proper tau phosphorylation by potentially circumventing the formation of overreactive Cdk5/p25 [37]. Effective therapies for tauopathies may require inhibition of both Cdk5/p25 and GSK3β. AF710B fulfills this condition, and because it decreased all tested phosho-tau isoforms including PHF-1, it may be effective as a disease modifier even in more advanced stages of AD and also for other taoupathies. Overall, our data indicates that AF710B decreases tau pathology and may restore synaptic homeostasis by decreasing p25 and inhibiting GSK3β and Cdk5 activities.

In summary we identified AF710B as a novel comprehensive therapeutic agent to ameliorate cognitive deficits, synaptic loss, amyloid and tau pathologies, neuroinflammation, and neurodegeneration in AD and perhaps additional related protein aggregation diseases. AF710B appears to be a highly effective treatment for AD, when compared with competing drugs (Table 2 A,B). A drug like AF710B that works in extremely low doses provides far more dosing and testing options for future Alzheimer’s disease therapeutics.

Acknowledgments

This study was supported by grants from the National Institute of Health (NIH): National Institute on Aging (NIA) P50-AG016573 (FML) and AG027544 (FML and RM) and National Institute of Neurological Disorders and Stroke (NINDS) R01NS080152 (IB) and F32NS093786 (DR). Dr. Ilya Bezprozvanny is a holder of the Carl J. and Hortense M. Thomsen Chair in Alzheimer's Disease Research. We thank Dr. Takaomi Saido (RIKEN Brain Science Institute, Wako-shi, Saitama, Japan) for providing APP-knockin mice. We thank Dr. Menahem Segal (Weizmann Institute of Science, Rehovot, Israel) for his advice and suggestions.

Abbreviations

AD	Alzheimer’s disease
Aβ	β-amyloid
APP-KI	Amyloid Precursor Protein-knockin
BACE1	Beta-Secretase1
CREB	cAMP response element binding protein
CDK5	Cyclin-Dependent Kinase 5
ER	endoplasmic reticulum
ERK 1/2	extracellular signal regulated kinase
ip	intraperitoneal
GPCR	G-protein coupled receptor

GSK3β	Glycogen Synthase Kinase 3β
M1 mAChR	M1 Muscarinic acetylcholine receptor
M1 PAM	M1 positive allosteric modulator
MWM	Morris water maze
PA	Passive Avoidance
po	per os
PP2A	Protein Phosphatase 2A
PS1-KI	Presenilin1-knockin
σ1R	Sigma-1 receptor
3xTg-AD mice	triple transgenic AD mice

References

1. Fisher A. Cholinergic treatments with emphasis on M1 muscarinic agonists as potential disease-modifying agents for Alzheimer's disease. Neurotherapeutics. 2008; 5:433–442. [PubMed: 18625455]
2. Fisher A. Cholinergic modulation of amyloid precursor protein processing with emphasis on M1 muscarinic receptor: perspectives and challenges in treatment of Alzheimer's disease. J Neurochem. 2012; 120:22–33. [PubMed: 22122190]
3. Caccamo A, Oddo S, Billings LM, Green KN, Martinez-Coria H, Fisher A, LaFerla FM. M1 receptors play a central role in modulating AD-like pathology in transgenic mice. Neuron. 2006; 49:671–682. [PubMed: 16504943]
4. Medeiros R, Kitazawa M, Caccamo A, Baglietto-Vargas D, Estrada-Hernandez T, Cribbs DH, Fisher A, LaFerla FM. Loss of muscarinic M1 receptor exacerbates Alzheimer's disease-like pathology and cognitive decline. Am J Pathology. 2011; 179:980–991.
5. Kourrich S, Su TP, Fujimoto M, Bonci A. The sigma-1 receptor: roles in neuronal plasticity and disease. Trends Neurosci. 2012; 35:762–771. [PubMed: 23102998]
6. Su TP, Hayashi T, Maurice T, Buch S, Ruoho AE. The sigma-1 receptor chaperone as an inter-organelle signaling modulator. Trends Pharmacol Sci. 2010; 31:557–566. [PubMed: 20869780]
7. Mishina M, Ohyama M, Ishii K, Kitamura S, Kimura Y, Oda K, Kawamura K, Sasaki T, Kobayashi S, Katayama Y, Ishiwata K. Low density of sigma1 receptors in early Alzheimer's disease. Ann Nucl Med. 2008; 22:151–156. [PubMed: 18498028]
8. Hayashi T, Tsai SY, Mori T, Fujimoto M, Su TP. Targeting ligand-operated chaperone sigma-1 receptors in the treatment of neuropsychiatric disorders. Expert Opin Ther Targets. 2011; 15:557–577. [PubMed: 21375464]
9. Jin JL, Fang M, Zhao YX, Liu XY. Roles of sigma-1 receptors in Alzheimer's disease. Int J Clin Exp Med. 2015; 8:4808–4820. [PubMed: 26131055]
10. Lahmy V, Meunier J, Malmström S, Naert G, Givalois L, Kim SH, Maurice T. Blockade of Tau hyperphosphorylation and Aβ1–42 generation by the aminotetrahydrofuran derivative ANAVEX2-73, a mixed muscarinic and σ1 receptor agonist, in a nontransgenic mouse model of Alzheimer's disease. Neuropsychopharmacol. 2013; 38:1706–1723.
11. Hayashi T, Su TP. Sigma-1 receptor chaperones at the ER-mitochondrion interface regulate Ca2+ signaling and cell survival. Cell. 2007; 131:596–610. [PubMed: 17981125]
12. Navarro G, Moreno E, Aymerich M, Marcellino D, McCormick PJ, Mallol J, Cortés A, Casadó V, Canela EI, Ortiz J, Fuxe K, Lluís C, Ferré S, Franco R. Direct involvement of sigma-1 receptors in the dopamine D1 receptor-mediated effects of cocaine. Proc Natl Acad Sci U S A. 2010; 107:18676–18681. [PubMed: 20956312]

13. Navarro G, Moreno E, Bonaventura J, Brugarolas M, Farré D, Aguinaga D, Mallol J, Cortés A, Casadó V, Lluís C, Ferre S, Franco R, Canela E, McCormick PJ. Cocaine inhibits dopamine D2 receptor signaling via sigma-1-D2 receptor heteromers. PLoS One. 2013; 8:e61245. [PubMed: 23637801]
14. Alonso G, Phan VL, Guillemain I, Saunier M, Legrand A, Anoal M, Maurice T. Immunocytochemical localization of the sigma 1 receptor in the adult rat central nervous system. Neuroscience. 2000; 97:155–170. [PubMed: 10771347]
15. Mavlyutov TA, Epstein ML, Andersen KA, Ziskind-Conhaim L, Ruoho AE. The sigma-1 receptor is enriched in postsynaptic sites of C-terminals in mouse motoneurons. An anatomical and behavioral study. Neurosci. 2010; 167:247–255.
16. Sun S, Zhang H, Liu J, Popugaeva E, Xu NJ, Feske S, Bezprozvanny I. Reduced synaptic STIM2 expression and impaired store-operated calcium entry cause destabilization of mature spines in mutant presenilin mice. Neuron. 2014; 82:79–93. [PubMed: 24698269]
17. Zhang H, Wu L, Pchitskaya E, Zakharova O, Saito T, Saido T, Bezprozvanny I. Neuronal store-operated calcium entry and mushroom spine loss in APP knock-in mouse model of Alzheimer's disease. J Neuroscience. 2015a in press.
18. Guo Q, Fu W, Sopher BL, Miller MW, Ware CB, Martin GM, Mattson MP. Increased vulnerability of hippocampal neurons to excitotoxic necrosis in presenilin-1 mutant knock-in mice. Nat Med. 1999; 5:101–106. [PubMed: 9883847]
19. Saito T, Matsuba Y, Mihira N, Takano J, Nilsson P, Itohara S, Saido TC. Single App knock-in mouse models of Alzheimer's disease. Nat Neurosci. 2014; 17:661–663. [PubMed: 24728269]
20. Zhang H, Liu J, Sun S, Pchitskaya E, Popugaeva E, Bezprozvanny I. Calcium signaling, excitability, and synaptic plasticity defects in a mouse model of Alzheimer's disease. J Alzheimers Dis. 2015b; 45:561–580. [PubMed: 25589721]
21. Oddo S, Caccamo A, Shepherd JD, Murphy MP, Golde TE, Kayed R, Metherate R, Mattson MP, Akbari Y, LaFerla FM. Triple-transgenic model of Alzheimer's disease with plaques and tangles: intracellular Abeta and synaptic dysfunction. Neuron. 2003; 39:409–421. [PubMed: 12895417]
22. Sur C, Mallora PJ, Wittmann M, Jacobson MA, Pascarella D, Williams JB, Brandish PE, Pettibone DJ, Scolnick EM, Conn PJ. N-desmethylclozapine, an allosteric agonist at muscarinic 1 receptor, potentiates N-methyl-D-aspartate receptor activity. Proc Natl Acad Sci U S A. 2003; 100:13674–13679. [PubMed: 14595031]
23. Davie BJ, Christopoulos A, Scammells PJ. Development of M1 mAChR allosteric and bitopic ligands: prospective therapeutics for the treatment of cognitive deficits. ACS Chemical Neurosci. 2013; 4:1026–1048.
24. Bradley SR, Lameh J, Ohrmund L, Son T, Bajpai A, Nguyen D, Friberg M, Burstein ES, Spalding TA, Ott TR, Schiffer HH, Tabatabaei A, McFarland K, Davis RE, Bonhaus DW. AC-260584, an orally bioavailable M(1) muscarinic receptor allosteric agonist, improves cognitive performance in an animal model. Neuropharmacology. 2010; 58:365–373. [PubMed: 19835892]
25. Davis AA, Heilman CJ, Brady AE, Miller NR, Fuerstenau-Sharp M, Hanson BJ, Lindsley CW, Conn PJ, Lah JJ, Levey AI. Differential effects of allosteric M1 muscarinic acetylcholine receptor agonists on receptor activation, arrestin 3 recruitment, and receptor downregulation. ACS Chemical Neurosci. 2010; 1:542–551.
26. Impey S, Obrietan K, Storm DR. Making new connections: role of ERK/MAP Kinase signaling in neuronal plasticity. Neuron. 1999; 23:11–14. [PubMed: 10402188]
27. Rosenblum K, Futter M, Jones M, Hulme EC, Bliss TVP. ERK I/II regulation by the muscarinic acetylcholine receptor in neurons. J Neurosci. 2000; 20:977–985. [PubMed: 10648702]
28. Roldan G, Bolanos BE, Gonzales SH, Quirarte GL, Prado AR. Selective M1 muscarinic receptor antagonists disrupt memory consolidation of inhibitory avoidance in rats. Neurosci Lett. 1997; 230:93–96. [PubMed: 9259472]
29. Senda T, Matsuno K, Okamoto K, Kobayashi T, Nakata K, Mita S. Ameliorating effect of SA4503, a novel sigma-1 receptor agonist, on memory impairments induced by cholinergic dysfunction in rats. Europ J Pharmacol. 1996; 315:1–10.
30. Hudkins RL, DeHaven-Hudkins DL. M1 muscarinic antagonist interact with sigma recognition sites. Life Sci. 1991; 49:1229–1235. [PubMed: 1658507]

31. Querfurth HW, LaFerla FM. Alzheimer's disease. N Engl J Med. 2010; 362:329–344. [PubMed: 20107219]
32. Ishikawa M, Sakata M, Ishii K, Kimura Y, Oda K, Toyohara J, Wu J, Ishiwata K, Iyo M, Hashimoto K. High occupancy of sigma1 receptors in the human brain after single oral administration of donepezil: a positron emission tomography study using [11C]SA4503. Int J Neuropsychopharmacol. 2009; 12:1127–1131. [PubMed: 19573265]
33. Tsai SY, Hayashi T, Harvey BK, Wang Y, Wu WW, Shen RF, Zhang Y, Becker KG, Hoffer BJ, Su TP. Sigma-1 receptors regulate hippocampal dendritic spine formation via a free radical-sensitive mechanism involving Rac1xGTP pathway. Proc Natl Acad Sci U S A. 2009; 106:22468–22473. [PubMed: 20018732]
34. Su SC, Tsai LH. Cyclin-Dependent Kinases in Brain Development and Disease. Annu Rev Cell Dev Biol. 2011; 27:465–491. [PubMed: 21740229]
35. Patrick GN, Zukerberg L, Nikolic M, de la Monte S, Dikkes P, Tsai LH. Conversion of p35 to p25 deregulates Cdk5 activity and promotes neurodegeneration. Nature. 1999; 402:615–622. [PubMed: 10604467]
36. Chow HM, Guo D, Zhou JC, Zhang GY, Li HF, Herrup K, Zhang J. CDK5 activator protein p25 preferentially binds and activates GSK3β. Proc Natl Acad Sci U S A. 2014; 111:E4887–E4895. [PubMed: 25331900]
37. Tsai SY, Pokrass MJ, Klauer NR, Nohara H, Su TP. Sigma-1 receptor regulates Tau phosphorylation and axon extension by shaping p35 turnover via myristic acid. Proc Natl Acad Sci U S A. 2015; 112:6742–6747. [PubMed: 25964330]
38. Medeiros R, Chabrier MA, LaFerla FM. Elucidating the triggers, progression, and effects of Alzheimer’s disease. J Alzheimers Dis. 2013; 33:S195–S210. [PubMed: 22635105]
39. Barron AM, Garcia-Segura LM, Caruso D, Jayaraman A, Lee JW, Melcangi RC, Pike CJ. Ligand for translocator protein reverses pathology in a mouse model of Alzheimer's disease. J Neurosci. 2013; 33:8891–8897. [PubMed: 23678130]
40. McKee AC, Carreras I, Hossain L, Ryu H, Klein WL, Oddo S, LaFerla FM, Jenkins BG, Kowall NW, Dedeoglu A. Ibuprofen reduces Aβ hyperphosphorylated tau and memory deficits in Alzheimer mice. Brain Res. 2008; 1207:225–236. [PubMed: 18374906]

A

Receptogram	K_H, nM	K_L, µM	Comments
M1 mAChR	0.046 (30%)	41	AF710B binds with high affinity to M1 mAChR showing an allosteric agonistic profile
σ1R	1.3 (19%)	0.25	AF710B binds with high affinity to σ1R and does not bind to σ2R (IC50>> 10µM)
Other		>/ 10	The high selectivity of AF710B for M1 mAChR & σ1R was shown in a high-throughput profiling that consists of a broad collection of 83 transmembrane (including GPCRs) and soluble receptors, channels and monoamine transporters *[Additional binding at 10µM to: M2 mAChR; 5 HT2A, 5HT2B, 5HT2C Receptors; Histamine 2 Receptor; 5HT Transporter. Inactive as agonist or antagonist at 10µM on histamine 2 and 5HT2A & 5HT2C receptors and a weak agonist at mu receptor (EC50=13µM); No effect on α4β2 and α7 nicotinic receptors, respectively].*

B

Efficacy index (K_L/K_H)	K_L, µM	K_H, nM	N	Compound
110	7.7	70 (37%)	6	Carbachol
1650	1.65	1 (27%)	6	Carbachol & AF710B, 0.1 nM

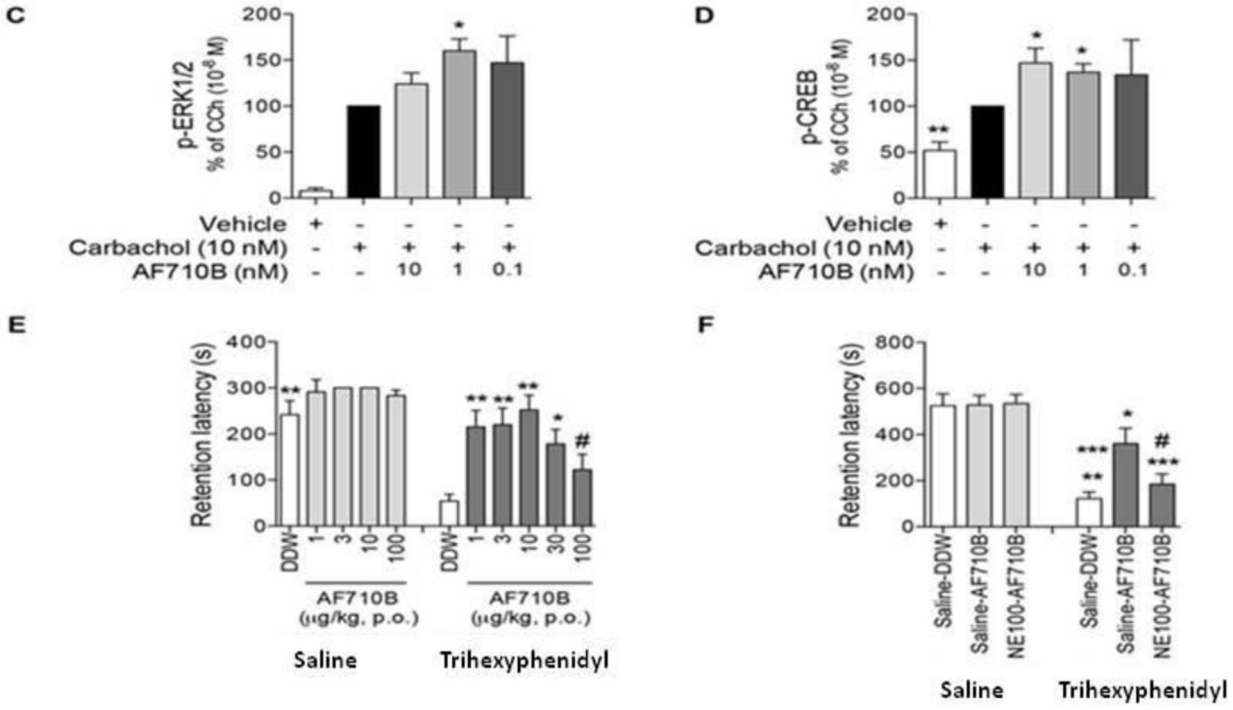

Figure 1. AF710B is a selective ligand for M1 mAChR and σ1R, potentiates the effects induced by carbachol and improves cognition in a passive avoidance test in trihexyphenidyl-treated rats

(**A**) In high-throughput receptogram profiling AF710B emerged as a highly selective ligand for M1 mAChR and σ1R, respectively as shown by displacement of tritiated-pirenzepine (an M1 mAChR radioligand) from rat cerebral cortex and tritiated-pentazocine (a σ1R radioligand) from guinea-pig cerebral cortex. (**B**) Very low concetrations of AF710B potentiates both carbachol-induced displacement of tritiated-pirenzepine from rat cerebral cortex and the efficacy of carbachol as evidenced by the ratio of K_L/K_H. (**C**) Very low concentrations of AF710B potentiated carbachol-induced phospho-Extracellular-signal-regulated kinases (pERK1/2) in starved proliferated PC12M1 cells. *p<0.001 vs. carbachol, 10 nM. (**D**) Very low concentrations of AF710B potentiated carbachol-induced phospho-CREB (cAMP response element-binding) in starved proliferated PC12M1 cells. **p< 0.001, *p<0.01 vs. carbachol, 10nM. (**E**) AF710B reverts the cognitive decline induced by trihexyphenidyl, an M1 mAChR antagonist. In *Experiments 1 and 2* the retention latencies

of trihexyphenidyl -treated rats with double distilled water (DDW) were significantly shorter than that of control rats treated with DDW ($p<0.001$). *Experiment 1 and 2* were combined as no significant differences were observed between the trihexyphenidyl-treated rats with DDW in both experiments. The retention latency of trihexyphenidyl- treated rats with AF710B (1, 3, 10 μg/kg, po) and AF710B (30 μg/kg, po) were significantly longer than that of trihexyphenidyl-treated rats with DDW. The retention latency of trihexyphenidyl-treated rats with AF710B 100 μg/kg, po was not different from that of trihexyphenidyl-treated rats with DDW. *$p<0.01$, **$p<0.001$, compared to trihexyphenidyl + DDW.#$p<0.01$, compared to trihexyphenidyl + 100 μg/kg, po of AF710B. (**F**) Retention latency of trihexyphenidyl-treated rats with DDW was significantly shorter than that of control rats treated with ($p<0.001$). The retention latency of trihexyphenidyl-treated rats with AF710B 10μg/kg was significantly longer and the σ1R antagonist NE 100 blocks the effects of AF710B. # $p< 0.02$, vs Saline + AF710B + Trihexyphenidyl; * $p<0.05$, vs. Saline + AF710B + Saline; ** $p<0.01$, vs. Saline + AF710B + Trihexyphenidyl; *** $p< 0.001$, vs. Saline+ DDW+ Saline; ***$p< 0.001$, vs. NE-100 + AF710B + Saline.

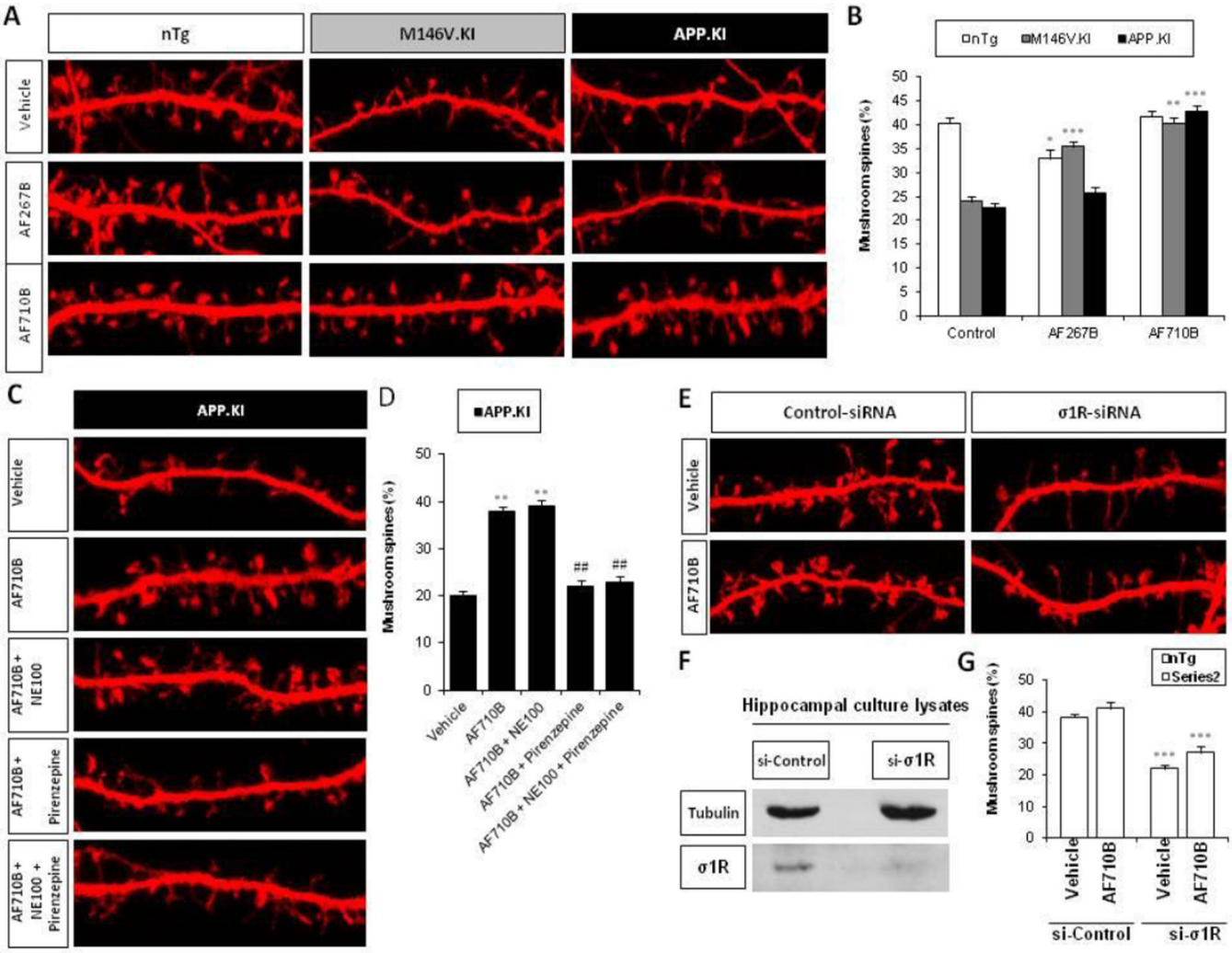

Figure 2. Activation of M1 mAChR/σ1R complex by AF710B restores synaptic spines

(**A–B**) Primary hippocampal neuron cultures were prepared from wild type non-transgenic (nTg), PS1-M146V-KI (M146V.KI) and APP-KI (APP.KI) pups. Hippocampal neurons were transfected with TdTomato to visualize dendritic spine morphology. By DIV16 the prevalence of mushroom spines decreased in both AD models relative to wild type cultures. 16-hour treatment of cultures with 30 nM AF710B prevented the loss of mushroom spines, whereas AF267B (1μM) was only partially effective in M146V.KI cultures. (**C–D**) In APP.KI cultures, the spine rescue by AF710B was unaffected by the σ1R antagonist NE100 (1 μM). Pirenzepine (1 μM) completely blocked the spine rescue by AF710B. The addition of NE100 had no additional effect. (**E–G**) Wild type hippocampal neuron cultures were transfected by lenti-viruses on DIV8 with plasmids encoding siRNA against σ1R (or scrambled siRNA as a control). Cells were harvested for western blotting on DIV17 to verify σ1R knockdown (**F**). (**E,G**) σ1R knockdown reduced the prevalence of mushroom spines to similar levels as in AD models. AF710B was unable to rescue mushroom spine loss from σ1R knockdown. *p<0.05, **p<0.001 and ***p<0.0001 in comparison to the respective control condition. $^{\#\#}$p<0.001 in comparison to AF710B.

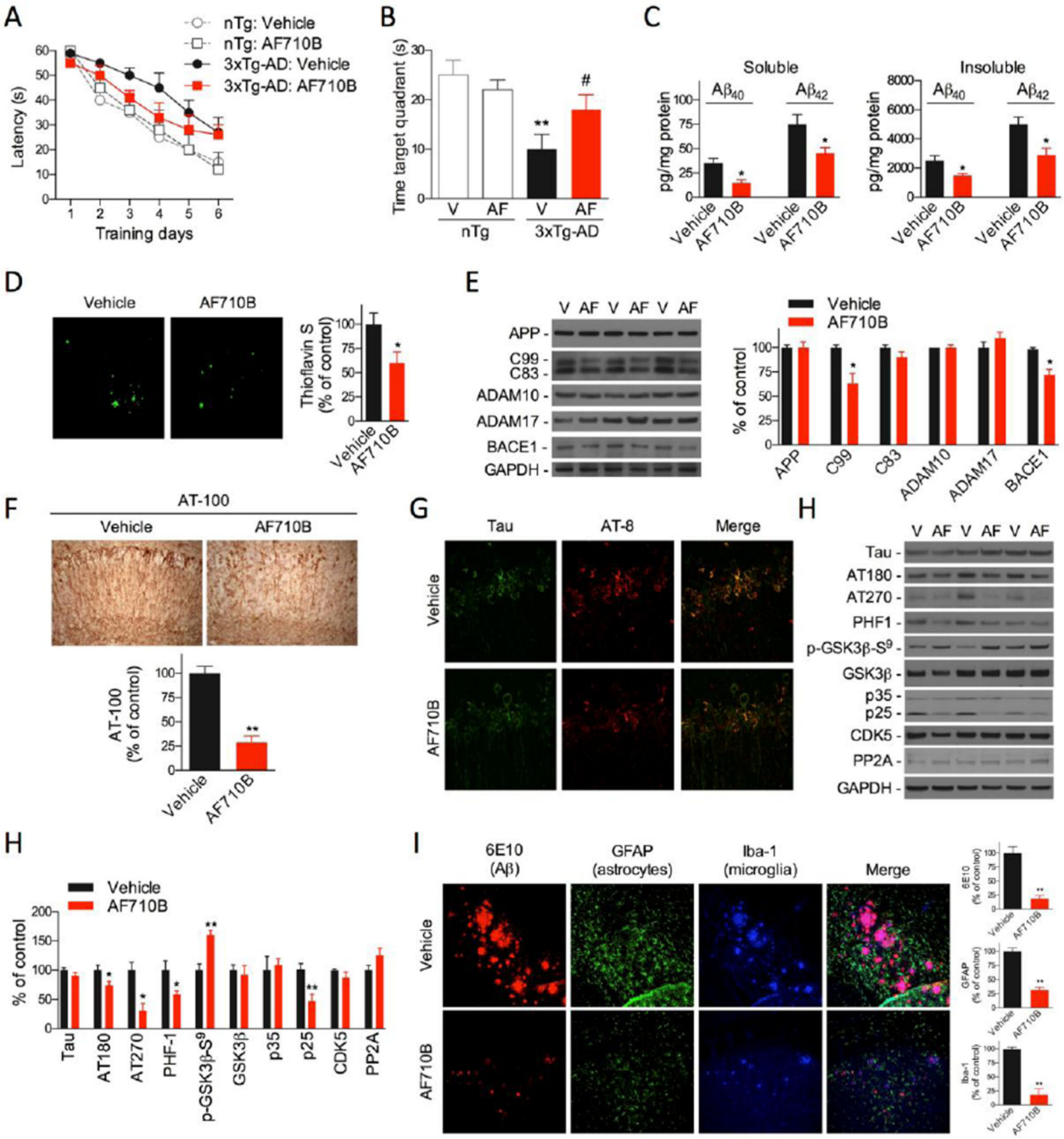

Figure 3. AF710B reduces AD-like pathology in the 3xTg-AD mouse model

(**A,B**) AF710B (10 μg/kg/day, ip) improves cognition in 12-month old 3xTgAD mice, as demonstrated by the (**A**) decrease in escape latency times to the platform, but not on the 6th day and (**B**) increase in the amount of time in the target quadrant compared to vehicle-treated 3xTgAD during the probe trial, in the Morris water maze. **P<0.01 between vehicle-treated nTg and 3xTgAD mice, #p< 0.05 between vehicle- and AF710B-treated 3xTgAD mice. (**C**) ELISA analysis reveals that levels of soluble and insoluble $A\beta_{40}$ and $A\beta_{42}$ are decreased in in 3xTgAD treated with AF710B (10 μg/kg/day). (**D**) Thioflavin S-

positive plaques are also reduced in AF710B-treated 3xTgAD mice, as shown by staining and volumetric analysis. (**E**) BACE1 and the C-terminal fragment of BACE cleavage of APP, C99, are significantly decreased in AF710B-treated 3xTgAD mice, while full-length APP and non-amyloidogenic enzymes ADAM10 and ADAM17 remain unchanged. Quantification of western blots was performed by densiometric analysis and is presented as a percentage of control, normalized to GAPDH. Activation of M1R/σ1R complex also reduces the phosphorylation of tau in the (**F**) AT-100 and (**G**) AT-8 epitopes in the 3xTg-AD mouse model. AF710B treatment results in the reduction of several phosphoepitopes of tau, while total tau levels remain the same in versus vehicle-treated 3xTgAD mice. (**H**) The reduction in tau phosphorylation seen in AF710B-treated 3xTgAD mice is mediated through GSK3β and CDK5, as demonstrated by the higher phosphorylation at Ser^{9} of GSK3β and reduced levels of the CDK5 activator peptide p25, respectively. Quantification of western blots was performed by densiometric analysis and is presented as a percentage of control, normalized to GAPDH. (**I**) AF710B reduces inflammation, as we found significant reduction in the number of $GFAP^{+}$-astrocytes and $Iba\text{-}1^{+}$-microglia in the vicinity of $6E10^{+}$-plaques. Graphs represent the volumetric analysis of Aβ, astrocytes and microglia. *P<0.05 and **P<0.01 between vehicle- and AF710B-treated 3xTgAD mice.

Table 1

AF710B: A compilation of neurochemical, behavioral and toxicological studies (re also Figs 1–3)

Effects of AF710B	Results	Comments
Receptogram	Re Fig 1A	Highly potent and selective for M1 mAChR and σ1R. Several effects mediated by M1 mAChR and σ1R and were detected at concentrations in the nM range which are lower by 3–4 orders of magnitude vs. interactions with any of the other tested screen of GPCRs, ion channels and transporters (Fig 1A). The M1 PAM brucine potentated the binding of orthosteric agonists (carbachol and AF267B) but not of AF710B; *not shown*. Thus AF710B is an M1 allosteric agonist.
Selectivity for M1–M5 mAChR in CHO cells; $[Ca^{2+}]_i$ readout	AF710B is a partial agonist at 100μM, inactive at 1μM. Selective for M1 mAChR with no agonistic activity on M2–M5 mAChRs. Enatioselectivity: AF710A is a M1 muscarinic antagonist *(not shown)*.	The M1 PAM brucine potentated the effects of the orthosteric agonists (carbachol and AF267B but not the effects of AF710B and TBPB (an M1 allosteric agonist); *(not shown)*. Thus AF710B is an M1 allosteric agonist *(not shown)*.
Potentiation of effects of carbachol (CCh) on M1 mAChR	Potentiates CCh binding and efficacy (Fig 1B) and CCh-mediated increase of p-ERK and p-CREB (Fig 1C& 1D)	Thus AF710B is a M1 PAM. Notably, AF710B differs from other M1 PAMs as it does not potentiate CCh-induced elevation of $[Ca^{2+}]_i$ in CHO-M1 cells *(not shown)*.
Tau phosphorylation	Decreased tau phosphorylation in NGF-deprived and Aβ25–35 -induced tau phosphorylation; effective at 100 μM-1nM	M1 mAChR -mediated (e,g. blocked by atropine; detected in PC12M1 cells but not in PC12 cells devoid of M1 mAChR); *(not shown)*.
GSK-3β activity	Increased inactive form of GSK3β in NGF-deprived and Aβ25–35-induced decrease of inactive form of GSK3β; effective at: 100 μM-1nM	M1 mAChR -mediated (e,g. blocked by atropine; detected in PC12M1 cells but not in PC12 cells devoid of M1 mAChR); *(not shown)*.
Neuroprotection; Bcl-2, Bax readouts	Neuroprotective against insults such as Aβ25–35 -induced neurotoxicity; NGF-withdrawal, effective at: 1μM-1nM	These effects of AF710B are not modulated by the M1 mAChR as can be observed both in PC12M1 and PC12 cells. AF710B-induced effects on Bax are mediated by σ1R (e.g. blocked by NE100) *(not shown)*.
Mushroom spine stability	AF710B rescued mushroom spines in hippocampal neuron cultures from PS1.KI and APP.KI mice. This was prevented by the M1 mAChR antagonist pirenzepine, but not the σ1R antagonist NE100. σ1R knockdown lead to mushroom spine loss in wild type hippocampal neurons. AF710B was unable to rescue this. AF267B also partially prevented mushroom spine loss in PS1.KI, but was ineffective in APP.KI cultures. Fig 2 A–F.	This indicates that the presence of σ1R and function of M1 mAChR are required for hippocampal neuron mushroom spine stability, suggesting that AF710B may target an M1 mAChRσ1R complex. Rescue of mushroom spines by AF710B may explain its ability to improve cognitive performance in spatial memory tasks. The less effective rescue of mushroom spines by AF267B suggests that targeting M1 mAChR function alone may not be sufficient to reverse some of the AD pathologies in AD.
Trihexyphenidyl-induced cognitive impairment in PA test in rats	Significantly effective at 1–30 μg/kg, po (Fig 1E); The effects of AF710B are mediated at least in part by σ1R (e.g. blocked by NE100; Fig 1F)	AF710B is the most potent cognitive enhancer [e.g. Donepezil, AF267B, AF292, AF102B, AF710A; re Table 2] Wide safety margin (> 50,000). Enantioselectivity: AF710A (10 and 1 μg/kg, po) is inactive (*not shown*).
3xTg-AD mice	Fig 3	AF710B was highly potent in restoring cognitive decline associated with AD and with lessening BACE1, GSK3β activity, p25CDK5, neuroinflammation, soluble and insoluble Aβ40, Aβ42, accumulation of amyloid plaques and neurofibrillary tangles.
Acute Toxicity (rats)	No toxic or side effects (highest tested dose, 50 mg/kg, po); no gross pathological changes at necropsy	MTD > 50 mg/kg, po *(not shown;* Male and Female Sprague-Dawley™ rats *GLP study Harlan, Israel)*.

Table 2

Compilation of data obtained with different compounds in:

(A) trihexyphenidyl-treated PA test in rats (all these studies were perfomed at IIBR under the same experimental protocol and therefore can be compared).									
	Compound (mg/kg, po) tested in the trihexyphenidyl-treated rats in PA								
Compound ***[Mechanism of action]***	**0.001**	**0.003**	**0.01**	**0.03**	**0.05**	**0.1**	**0.5**	**1**	**Safety Margin (Toxic/effective dose)**
AF710B *Mw 357.5* *[M1 allosteric agonist/ σ1R agonist]*	P	P	P	P		N			50000
AF710A Mw 357.5 *Enantiomer of AF710B*	N		N						Not applicable
AF102B (*aka* Cevimeline) *Mw 235* *[M1> M3 orthosteric agonist]*								P	115
AF267B *Mw 214* *[M1 orthosteric agonist]*			N		P	P	P	P	400
AF292 *Mw 199* *[M1 orthosteric agonist]*				N	P	P	P	P	3300
Donepezil (*aka* Aricept) *Mw 416* *[σ1R agonist/AChE-I]*						N		N	Not applicable
Donepezil (0.1mg/kg, po) *[σ1R agonist/AChE-I]* + AF267B *[M1 orthosteric agonist]*					P	P			Not applicable

(B) in the 3xTg-AD mice [38–40].					
Intervention in 3xTgAD mice	**Aβ**	**tau**	**Inflammation**	**Effection Cognition**	**Dose**
AF710B	↓	↓	↓	↑	**10 μg/kg/day, i.p., 2 months**
Anti-IL-1R antibody	↓	↓	↓	↑	**200 μg/every 8–9 d, i.p., 6 months**
Calpain inhibitor (A-705253)	↓	↓	↓	↑	**80 mg/kg/day, p.o., 3 months**

(B) in the 3xTg-AD mice [38–40].					
Intervention in 3xTgAD mice	**Aβ**	**tau**	**Inflammation**	**Effection Cognition**	**Dose**
α7 nicotinic agonist (A-582941)	No change (NC)	NC	NC	↑	**12 mg/kg/day, p.o., 3 months**
TSPO ligand (Ro5-4864)	↓	**NC**	↓	↑	**3 mg/kg/once weekly, ip., 3 months**
Ibuprofen	↓	↓	Not Tested (NT)	↑	**375 ppm on chow, 4 months**
Lithium	NC	↓	NT	NC	**300 μl of 0.6 mol/L LiCI/mouse/day, i.p., 4 weeks**
M_1R agonist (AF267B)	↓	↓	NT	↑	**3 mg/kg/day, i.p., 10 weeks**
Memantine	↓	↓	NT	↑	**30 mg/kg/day, i.p., 3 months**
Mifipristone	↓	↓	NT	↑	**1.2 mg/day, s.c., 21 days**
Nicotinamide	NC	↓	NT	↑	**200 mg/kg/day, p.o., 4 months**
Nicotine	NC	↑	NT	NT	**= 3 mg/day, p.o., 3 months**
Dexamethasone	↑	↑	NT	NT	**5 mg/kg/day, i.p., 7 days**

P = significant mitigation of cognitive deficit; N = No significant mitigation of cognitive deficit